ACS Sustainable Chemistry & Engineering

Research Article

pubs.acs.org/journal/ascecg

Oxidative Capacity of Nanobubbles and Its Effect on Seed Germination

Shu Liu,*[,†] Seiichi Oshita,*[,†] Yoshio Makino,[†] Qunhui Wang,[‡,§] Yoshinori Kawagoe,[∥] and Tsutomu Uchida[⊥]

[†]Graduate School of Agricultural & Life Sciences, The University of Tokyo, Yayoi 1-1-1, Bunkyo-ku, Tokyo 113-8657, Japan

[‡]Department of Environmental Engineering, School of Civil and Environmental Engineering, University of Science and Technology Beijing, 30 Xueyuan Road, Haidian District, Beijing 10083, China

[§]Beijing Key Laboratory on Resource-Oriented Treatment of Industrial Pollutants, University of Science and Technology Beijing, 30 Xueyuan Road, Haidian District, Beijing 10083, China

[∥]College of Bioresource Sciences, Nihon University, Kameino 1866, Fujisawa, Kanagawa 252-0880, Japan

[⊥]Division of Applied Physics, Faculty of Engineering, Hokkaido University, N13W8 Kita-ku, Sapporo, Hokkaido 060-8628, Japan

Supporting Information

ABSTRACT: Nanobubbles (NBs) have been reported to be effective at accelerating the metabolism of living organisms, but the mechanism is not yet well understood. In this study, the production of reactive oxygen species (ROS) by NBs and its effect on seed germinations were investigated. The fluorescence response of APF to NB water was measured. It changed depending on the NB number density which decreased with storage time. This indicated that NBs could produce ROS and the amount of ROS had positive correlation with the NB number density. The fluorescence intensity of APF increases linearly with the concentration of H_2O_2 in the range of 0−1 mM. Just after the NB generation, the oxidative capacities represented by amount of ROS of oxygen NB water and gas-mixture (air + nitrogen) NB water were estimated to be equivalent to 0.5 and 0.3 mM H_2O_2 respectively. The seed germination tests were performed in the NB water, distilled water and H_2O_2 solutions. The germination rate at each observation times of seeds submerged in gas-mixture NB water and 0.3 mM H_2O_2 solutions were both higher than those submerged in distilled water. The amounts of superoxide radicals in the seeds were detected using NBT staining. The results of absorbance data proved that the amounts of $O_2^{\bullet-}$ in seeds submerged in gas-mixture NB water and in 0.3 mM H_2O_2 solution were similar and significantly higher than those in the distilled water. These results indicated that moderate level of exogenous ROS produced by NB water played an important role in seed germination.

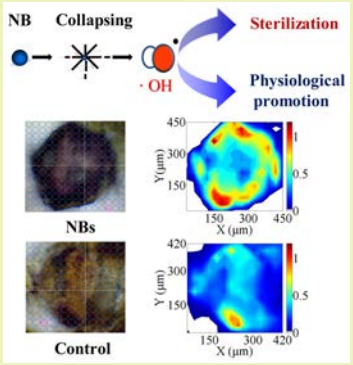

KEYWORDS: *Reactive oxygen species, Bubble number density, Microscope spectrophotometer, Hydrogen peroxide, Fluorescence intensity*

INTRODUCTION

Microbubbles (MBs) are bubbles with a diameter ranging from several micrometers to about 100 μm. Nanobubbles (NBs) are bubbles with a diameter of submicrometer order.[1] Since the 1990s, many types of commercial micro- and nanobubble (MNB) generators have been invented in Japan, such as swirl flow, ejector, cavitation, pore, mechanical agitation, and sonication.[2] These MNB generators can produce the water containing high number concentration of MNBs ranging from 10^6 to 10^8 particles/mL. MNBs show various characteristics such as the increased solubility of gases in liquids, reduced friction, either negative or positive ζ-potentials and the generation of free radicals.[3−5] Because of their unique properties, the MNBs application technology has widely been used in many fields.

Recently, MNB physiological promotion effect and oxidation effect have both been reported. A series of investigations have reported that water containing MNBs can accelerate the growth of plants, shellfish, and yeast.[6−10] On the other hand, MNBs are widely used to improve the oxidation effect.[11−16] For example, ozone MNBs are effectively used to remove residual pesticides in vegetables,[11,12] to inactivate microorganisms,[13] and to reduce the organic material in wastewater.[14−16] MNBs' oxidative promotion effects were not only due to the reason that MNBs can enhance the mass transfer of ozone but also that the exogenous reactive oxygen species (ROS) are generated by MNBs in the presence of dynamic stimuli such as ozone, strong acid, copper, and short-wavelength UV irradiation.[17−20]

The physiological promotion and oxidation effects of MNB water described above may seem contradictory to each other. However, the generation of reactive oxygen species (ROS) caused by NBs may offer a reasonable explanation for these two

Received: October 26, 2015
Revised: December 3, 2015
Published: December 11, 2015

DOI: 10.1021/acssuschemeng.5b01368
ACS Sustainable Chem. Eng. 2016, 4, 1347−1353

effects because excess concentration of ROS has oxidation effect and moderate concentration of ROS can show physiological promotion effect. As we know, ROS have long been regarded as damaging compounds. ROS can cause oxidative damage to macromolecules, thus leading to lipid peroxidation, DNA damage, and DNA breaks.[22,23] Owing to these principles, ROS are widely used in sterilization and oxidation processes. However, as has reported in recent year, ROS play a dual role in seed physiology behaving.[21] Appropriate amount of ROS does not act as harmful compounds but instead, it plays an important role as cell wall loosening factor and essential signaling molecules in the growing process of plant.[24,25] It has been accepted that exogenously supplied H_2O_2, a kind of ROS, can promote the germination of cereal plants such as barley, wheat, rice, and *Zinnia elegans* seeds.[26−28]

In our latest research on NBs, we reported that the germination rates of barley seeds submerged in NB water were 15−25% greater than those of seeds submerged in distilled water with the same concentration of DO.[29] According to this result and the dual roles of ROS described above, we hypothesize that without dynamic stimuli, NBs can also supply a small amount of exogenous ROS in the water. With this idea in mind we have studied the production of ROS by NB water using a fluorescent probes, 3′-*p*-(aminophenyl) fluorescein (APF). As the fluorescence response of APF to NB water changed with storage time, it is important to grasp the relationship between the amount of ROS and the NB number density in water. The fluorescence intensity of APF increases linearly with the concentration of H_2O_2 in the range of 0−1 mM. Therefore, the oxidative capacity of NB water was estimated using the correlation equation between the fluorescence intensities of APF and the concentrations of H_2O_2 solutions.

A second aim of this work was to study the role of exogenous ROS produced by NB water in the seed germination process. The germination tests were performed among the barley seeds submerged in the NB water, distilled water and different concentrations of H_2O_2 solutions under the similar DO concentrations. The amounts of superoxide radicals in the seeds submerged in the NB water, distilled water, and different concentrations of H_2O_2 solutions were detected using nitro blue tetrazolium (NBT) staining. We suppose that as signaling molecules, the exogenous ROS produced by NBs can play an important role in seed germination.

EXPERIMENTAL SECTION

Generation of NB Water. 2 L of distilled water was placed in an Erlenmeyer flask. The distilled water was produced in a distillation unit (Autostill WA-53, Yamato Scientific Co., Ltd., Japan), which is equipped with a water storage tank of 40 L capacity. The gas was introduced into the distilled water and circulated through a micro and nanobubble generator (OM4-GP-040, Aura Tec Co. Ltd., Japan) for 1 h at a constant temperature of 20 °C to obtain "water containing MNBs". The DO concentration of distilled water was about 8 mg L^{-1}. The DO concentrations of oxygen MNB water, air MNB water, and nitrogen MNB water were about 40, 12, and 0.04 mg L^{-1}, respectively. To adjust the DO concentration of MNB water to be the same as the distilled water, the gas-mixture of nitrogen (purity 99.999 95%, Taiyo Nippon Sanso Co. Ltd., Japan) and air (CO_2 < 1 ppm, THC < 1 ppm, Taiyo Nippon Sanso Co. Ltd., Japan) was used. The ratio of nitrogen and air was adjusted through a mixed-gas flow regulator (Log MIX-D100A-0050 and Log MIX-D100A-0052, FRONTO Co. Ltd., Japan). In this way, we can obtain the MNB water with a certain DO concentration in the range from 0.04 to 12 mg L^{-1}. During the MNB production, the water had a milky appearance. This appearance was observed just a few seconds after we started the MNB generation and it was maintained during the whole bubble generation period. When the MNB generation stopped, the milky appearance gradually vanished. In about 10 min, the water in the 2 L Erlenmeyer flask became transparent. Most of the MBs can exist in the water for only about 10 min, whereas NBs are relatively stable and can exist in the pure water for days.[29,30] Therefore, the expression of "gas-mixture NB water" is used in this paper. NB number densities were measured using the nanoparticle tracking analysis method (NanoSight-LM10, Quantum Design Inc., Japan). Using a laser-illuminated optical microscope, we observed NBs as light-scattering centers moving under Brownian motion. Bubble-size distributions were measured using the nanoparticle tracking analysis method, a kind of dynamic light scattering (NanoSight-LM10, Quantum Design Inc., Japan), which has been widely used to determine the sizes of nanoparticles in liquids.[31]

Production of ROS by NBs. APF (5 mM, Sekisui Medical Co., Ltd., Japan), a fluorescent reagent that is highly resistant to autoxidation, was used for detecting generation of ROS (mainly hydroxyl radicals, OH) by NBs.[32] APF itself has almost no fluorescence intensity. After APF reacts with ROS, fluorescein (with strong fluorescence intensity) is generated. Other chemicals were purchased from Kanto Chemical Co., Inc. and were of the highest obtainable purity. H_2O_2 solutions were prepared prior to each use. To obtain fluorescence excitation−emission matrixes (EEMs), excitation wavelengths were incrementally increased from 450 to 550 nm at 1 nm steps; for each excitation wavelength, the emission at longer wavelengths was also detected at 1 nm steps using a fluorescence spectrophotometer (F-7000, Hitachi High-Tech Co. Ltd., Japan). The fluorescein caused by ROS has an EEM peak located at excitation wavelength 490 nm and emission wavelength 515 nm. The slit width was 5 nm for both excitation and emission. The photomultiplier voltage was set at 800 V. The fluorescent intensity was given as a relative value corresponding to a combination of parameters' setting such as slit width, location of lamp, voltage, etc.

NBs were generated in 2 L of phosphate buffer (0.1 M, pH 7.4) without APF for 60 min at a constant temperature of 20 °C. NBs were formed with pure oxygen (purity 99.999 95%, Taiyo Nippon Sanso Co. Ltd., Japan) or gas-mixture (described in Generation of NB Water). Then the NBs solution was stored in the sealed biochemical oxygen demand (BOD) bottles. After a certain NB water storage time, 10 mL of buffer containing NBs was quantitatively taken out for each sample. Then 2 μL of APF was added for each sample, and the samples were measured for fluorescence intensities. The final concentration of APF was 1 μM. The control water is the phosphate buffer aerated with pure oxygen gas through a tube with an inner diameter of 4 mm. The DO concentration of this control water was around 40 mg L^{-1}, and few bubbles were observed using a laser-scattering image system (Zeecom, Microtech Co. Ltd., Japan).

To increase the disappearing speed of NBs number in the sample, a low intensity ultrasonic wave (150 W, 38 kHz) was applied to the control water and NBs water for 60 s. After the samples were taken out from the ultrasonic device, APF was added into each sample. Then the fluorescence intensities of the samples were measured.

Seed Material. Seeds of barley (*Hordeum vulgare* L.), which were harvested in 2012 and stored under controlled conditions (room temperature), were obtained from the University of Ehime, Japan. These seeds were screened with a magnifying lens, and only large seeds without visible defects were selected.

Germination Test. Germination tests were repeatedly performed with five seed groups. Each of them was composed of 100 barley seeds. Then every group was sealed in plastic net bags; one group was submerged in a 1 L beaker filled with water containing MNBs (the mixture of nitrogen and air was used to adjust the DO of MNB water to be the same as the distilled water), one in a beaker filled with distilled water and the others in beakers filled with different concentrations (0.1, 0.3, and 0.5 mM) of H_2O_2 solutions. During the germination experiments, to avoid the lack of oxygen and to

DOI: 10.1021/acssuschemeng.5b01368
ACS Sustainable Chem. Eng. 2016, 4, 1347−1353

maintain a certain amount of NBs in the water, NB water, distilled water, and H_2O_2 solutions were changed every 12 h. The MBs can only exist in water for about 10 min and then will disappear, so in germination experiments it is only NBs left in the water that are effective. Germination tests were performed at 20 °C in the dark. Germination rates obtained from three independent replicates are shown as mean ± standard deviation (SD).

Amount of Superoxide Radical in Seeds. Superoxide radicals (ROS, $O_2^{\bullet-}$) were detected and quantified by staining with nitrobluetetrazolium (NBT, Tokyo Chemical Industry Co., Ltd. Japan). After 17 and 37 h of submerging time, five germinated seeds in each group were incubated in a mixture of 1 mM NBT and 10 mM Tris−HCl buffer (pH 7.34) at room temperature for 30 min. Each seed was horizontally placed in a stainless steel cube container (15 × 15 × 15 mm). The sample containers were filled with super cryo-embedding medium (SCEM-L1, Section-lab Co. Ltd., Japan). The samples were rapidly frozen in an isopentane solution (Kanto chemical Co. Inc., Japan) at −105 °C for approximately 3 min. The prepared cube samples were fixed on the sample holder and stabilizedon the cryostat platform (Leica CM1950, Leica Biosystems Co. Ltd., Japan) for about 10 min. After the frozen samples were stabilized, they were attached to the cryostat stage one at a time. The working temperature for the cutting process was −20 °C. The longitudinal axis of each seed was vertical to the cutting knife direction (Surigipath DB80LS, Section-lab Co. Ltd., Japan). The cutting process was as follows. A 15 mm wide transparent adhesive film (Cryofilm type II C (9); Section-lab Co. Ltd., Japan) was laid on the sample surface and was firmly pressed to adhere to the cutting surface of the sample. The sample was then slowly cut into 100 μm slices continuously from the tip of the sprout. The film with the cut sample was placed on a glass slide with both the ends of the film section fastened with double sided adhesive tape. The measurement processes for superoxide radicals in seeds are shown in Figure S1.

Subsequently, the samples were measured spectrophotometrically. Superoxide radicals were visualized as deposits of dark blue insoluble formazan using a microscope spectrophotometer (MSV-5000, JASCO Co. Ltd., Japan). The microscope spectrophotometer uses UV−visible spectra, and the spectral analyses were conducted on each preset circle of 30 μm in diameter. The measured absorbance value is the average of the absorbance in each cycle area. The distribution of ROS inside the barley seed cells was determined using fixed wavelength measurements (absorbance difference between 560 and 700 nm), with absorbance at 560 nm representing the amount of dark-blue colored formazan. The difference in absorbance values at these wavelengths represents the amount of ROS at each location and also reduces the spectral background caused by impurities or radiation scattering.

After the maximum concentration of ROS in the sample was located by fixed wavelength measurements, spectrum measurements were conducted at the locations with the maximum concentration of $O_2^{\bullet-}$ in the samples from 450 to 700 nm with intervals of 1 nm. For each sample, we selected 5−12 measurement circles of 10 μm in diameter. The spectrum measurements were conducted at 450−700 nm at locations that showed a maximum amount of ROS.

RESULTS

NB Number Density. As can be seen in Figure 1, bubble-number densities increased with the MNB generation time. The geometric mean bubble size observed was around 108, 112, and 105 nm after 10, 30, and 60 min bubble generation, respectively. The total bubble-number densities of gas-mixture NBs were 0.41, 0.75, and 0.83 × 10^8 particles/mL after 10, 30, and 60 min bubble generation, respectively. These results showed that the mean bubble sizes will not change with the bubble generation time. But the bubble number density will increase with bubble generation time, and then get stable 30 min later. The following experiments were conducted with the 60 min generation NB water.

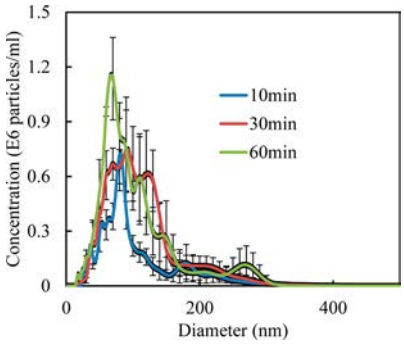

Figure 1. Bubble size distribution in the gas mixture NBs with different generation times (black error bars indicate standard error of the mean (n = 3)).

Production of Exogenous ROS by NBs. In the following experiments, the fluorescence response of APF to oxygen NB water was further studied to verify whether NBs can produce ROS in water. The fluorescent intensity of APF is corresponding to the amount of ROS in the water. As can be seen in Figure 2A, the fluorescence intensities of water

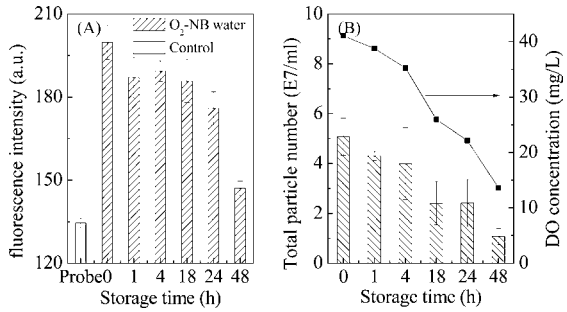

Figure 2. (A) Fluorescence response of 1 μM APF to oxygen NB water with water storage time. Fluorescence intensities were acquired in 0.1 M phosphate buffer at pH 7.4 (λ_{ex} 490 nm, λ_{em} 515 nm). Phosphate buffer was aerated with pure oxygen as the control whose DO concentration was above 40 mg L^{-1}. To obtain sufficient bubble number density, oxygen NBs generated for 1 h and then was stored in several biochemical oxygen demand (BOD) bottles. The error bars show the standard errors of 8 parallel samples. (B) Time course measurement for total bubble number concentrations and DO concentrations of oxygen NB water. The error bars show the standard errors of 3 measurements.

containing oxygen NBs were statistically higher than those of control water. With different NB water storage time, the fluorescence response of APF to oxygen NB water was measured. We found that the higher value of fluorescent intensities of oxygen NB water remained within the 2 day storage time, indicating that oxygen NBs can continuously produce a small amount of ROS. Furthermore, we found that the total NB number densities in the water were decreasing with storage time. After 2 day storage, the total NB number density was only 1/5 of the value just after the NB generation (Figure 2B). The DO concentration of oxygen NB water decreased from 40 to about 13 mg L^{-1} (Figure 2B). At the same time, the statistical differences between the fluorescence intensities of oxygen NB water and the control water gradually decreased from 60 to approximately 20. These results meant that the amount of ROS produced by NB water has positive correlation with the NB number density in the water. The nanoparticle tracking analysis cannot distinguish between NBs

DOI: 10.1021/acssuschemeng.5b01368
ACS Sustainable Chem. Eng. 2016, 4, 1347−1353

and foreign matters. However, the decrease of total particle number density proved that most of the particles that exist in the water are actually NBs rather than solid nanoparticles.

Compared to the oxygen NBs, the amount of ROS produced from the gas-mixture NBs which was used in the germination tests was relatively fewer. The fluorescent increase caused by gas-mixture NB water was about half of the oxygen NB water (Figure S1).

Oxidative Capacity of NBs in the Water. H_2O_2 is a weak ROS. Low concentration of H_2O_2 is mainly used as a cell signaling molecule but not an oxidizing substance.[33] The physiological promotion effects of NB water were similar to moderate concentrations of H_2O_2 solutions. Thus, we estimate the oxidative ability of NB water using H_2O_2 solutions. Under the same measuring conditions, the fluorescence response of APF to NB water and different concentrations of H_2O_2 were studied. In this way, we estimated the oxidative ability of water containing NBs by using the correlation equation between the fluorescence intensities of APF and the concentrations of H_2O_2 solutions. Different concentrations of H_2O_2 were added to the phosphate buffer solution, following which 1 μM APF was added. Figure 3A–D shows the contours of EEM spectrum of

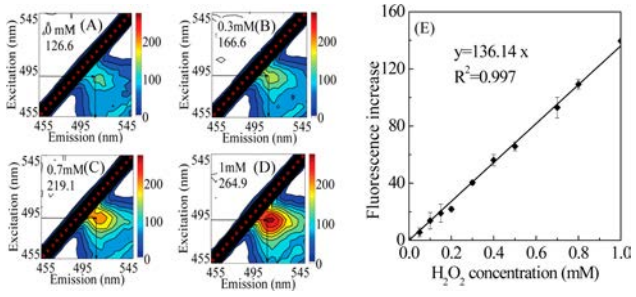

Figure 3. (A–D) Fluorescence response of 1 μM APF to H_2O_2 solution. EEM spectra were acquired in 0.1 M phosphate buffer at pH 7.4 (the fluorescence intensities were determined at 515 nm with excitation at 490 nm, slit width 5 nm). (E) Linear correlation between fluorescence increase and concentrations of H_2O_2 solution. The error bars show the standard errors of 3 parallel samples.

APF with different concentrations of H_2O_2 recorded from 450 to 550 nm in the emission wavelength and from 450 to 550 nm in the excitation wavelength. As indicated in Figure 3E, the fluorescence intensity of APF (λ_{ex} = 490 nm, λ_{em} = 515 nm) increased gradually upon the increase of H_2O_2 concentration. We observed a linear correlation between the fluorescence intensity and the concentration of H_2O_2. Just after NB generation, the fluorescence increase of APF solution caused by oxygen NB water was approximately 60. According to the formula, just after the NB generation, the oxidative capacity of oxygen NBs water is equivalent to 0.5 mM H_2O_2. Similarly, the oxidative capacity of gas-mixture NBs water is equivalent to 0.3 mM H_2O_2 (Figure S1).

Germination Tests. Then, we studied the role of exogenous ROS produced by NBs in the water in seed germination process. Table 1 shows the germination rates of barley seeds in response to different treatments at 20 °C. After 17 h submerging in the water, the average germination rate of barley seeds immersed in the gas-mixture NB water was 58%, which was 2 times higher than that in the distilled water. These results indicated that NBs effectively promoted the germination speed of barley seeds. In our experiments, low concentrations of H_2O_2 solutions were used as positive controls. As can be

Table 1. Germination of Barley Seeds at 20 °C in the Dark[a]

	germination rate (%)	
water type	17 h	37 h
distilled water	28 ± 0.9	98 ± 0.4
0.1 mM H_2O_2	48 ± 4.0	98 ± 0.4
0.3 mM H_2O_2	58 ± 4.0	100 ± 0
0.5 mM H_2O_2	54 ± 4.0	100 ± 0
NBs	58 ± 3.8	100 ± 0

[a]The DO concentrations of NBs water were adjusted to be the same as those of the distilled water. Data are means of three replicates ± SD. $P < 0.05$.

seen in Table 1, when the H_2O_2 concentrations were higher than 0.3 mM, they had a similar promotional effect on the germination speed of barley seeds as that of gas-mixture NB water. After 37 h of submerging time, although nearly 100% of the seeds in five groups (NB water, distilled water, H_2O_2 solutions of 0.1, 0.3, 0.5 mM) had germinated, the sprouting parts of barley seeds submerged in NB water were considerably larger than those in the other four groups (data not shown).

Superoxide radical in seeds. Various forms of ROS (e.g., superoxide radical, hydrogen peroxide, and hydroxyl radicals) exist in the seeds.[21] Among these, the production of superoxide radicals ($O_2^{\bullet-}$) is an important component for seed germination, seeding growth, and development.[34] The amount of superoxide radicals generated inside barley seeds was studied to explain the faster germination process caused by NBs and H_2O_2. The superoxide radical was detected and quantified using nitro blue tetrazolium (NBT) chloride. $O_2^{\bullet-}$ was visualized in the seeds using NBT, which produced formazan within the seed at the sites of $O_2^{\bullet-}$ formation.

Quantification of $O_2^{\bullet-}$ inside the seeds was achieved with the spectra from microscopic samples. Superoxide radical $O_2^{\bullet-}$ oxidized the yellow dye (NBT) to a blue colored formazan, which was measured spectrophotometrically at 560 nm.[24] The sprouts of barley seeds started to break the seed coat after 15–16 h submerging in the water, whereas after 37 h submerging time, nearly all the seeds germinated. Thus, we measured the $O_2^{\bullet-}$ inside barley seeds after 17 and 37 h submerging times, respectively. The concentrations of $O_2^{\bullet-}$ in the sprouting parts of seeds in the five groups were compared.

Figure 4 shows the superoxide radical distribution in barley seeds. According to the results of Figure 4, Figure 5 displays the spectra of formazan produced at the locations of a maximum amount of superoxide radical. The average level of endogenous ROS in the sprouting part of barley seeds germinated in different solutions were also calculated (Figure S3). It can be clearly observed that the concentrations of endogenous ROS in seeds after 17 h submerging time were much higher than those after 37 h, which means ROS were mainly produced just after the sprouts broke the seed coat (Figure 4, Figure S4, and Figure 5). The relative absorbance values at around 560 nm for the seeds which germinated in H_2O_2 solutions were significantly higher than those of distilled water after submerging for 17 and 37 h (Figure 5). The results above showed that the exogenous ROS (such as H_2O_2) in the water could stimulate the endogenous ROS production of barley seeds.

After 17 h of submerging, the concentrations of endogenous ROS of seeds that germinated in NB water were higher than all those that were submerged in the H_2O_2 solutions (Figure 5A). After 37 h of submerging, the concentrations of $O_2^{\bullet-}$ of seeds submerged in the gas-mixture NB water and H_2O_2 solutions

DOI: 10.1021/acssuschemeng.5b01368
ACS Sustainable Chem. Eng. 2016, 4, 1347–1353

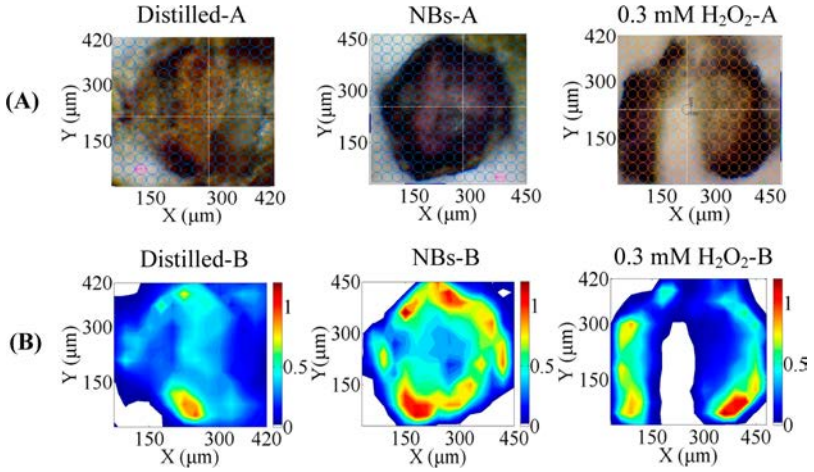

Figure 4. Superoxide radicals (ROS) distribution in barley seeds after 17 h of submerging time: the sprouting region of representative seeds germinated in three groups (distilled water, NB water, 0.3 mM H_2O_2) after the nitro blue tetrazolium staining process. (A) Microscopic images of the sectioned surfaces of seeds germinated in three different kinds of water. Spectra were conducted on each preset circle. The diameter of each circle is 30 μm. (B) Superoxide radical distribution in samples. The *x*- and *y*-axes show the locations of the measurement cycles. The measured values are the differences between absorbance values at 560 and 700 nm in each cycle area.

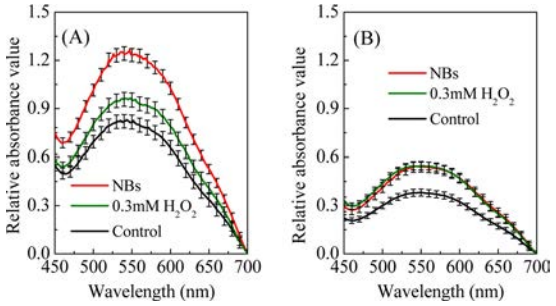

Figure 5. Spectra of formazan produced as a result of superoxide radical production in the sprouting region of germinated barley seeds immersed in distilled water, NB water, and 0.3 mM hydrogen peroxide solution. The measurements were conducted at locations with a maximum amount of ROS according to the fixed wavelength measurements described in Figure 4. For each group we measured five seeds. Each curve represents the mean value of more than 120 microscopic sample dots (dot diameter = 10 μm). (A) 17 h of submerging time. (B) 37 h of submerging time.

were similar (Figure 5B). According to our results, we conclude that gas-mixture NBs have similar or even higher effects on the endogenous ROS production compared with the H_2O_2 solutions used in this experiment.

DISCUSSION

Reactive oxygen species are often blamed as damaging compounds for the development of cancer and other diseases. However, in recent years scientists found that a moderate level of ROS may have beneficial effects. For example, in plant biological field, it is accepted that ROS plays a dual role in seed physiology behaving. Bailly et al.[21] raised a concept of the "oxidative window for germination", which restricts the occurrence of the cellular events associated with germination to a critical range of ROS level, enclosed by lower and higher limits. Below this window, the amount of ROS during imbibitions is too low for allowing germination. Above this window, ROS became deleterious and caused cellular oxidative damage. Owusu-Ansah and Banerjee[35,36] discovered that

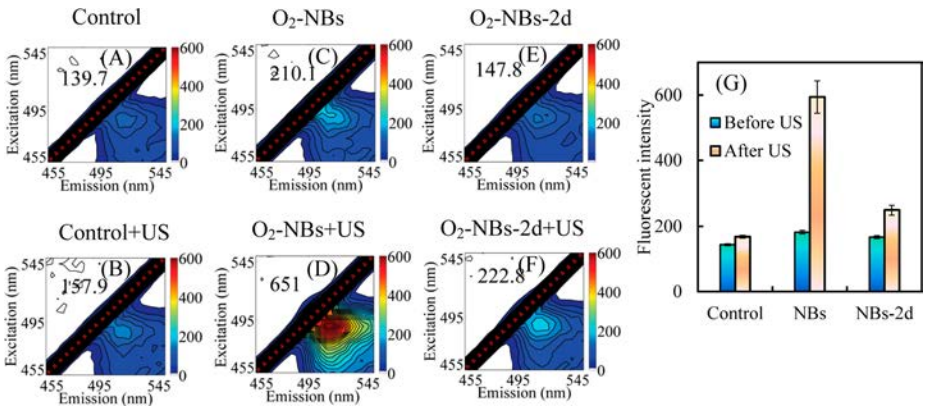

Figure 6. Effect of ultrasonic wave (US) on the fluorescent intensities of the buffer solutions with and without NBs ((A and B) EEM spectra of buffer solution without NBs (control) before and after US was applied; (C and D) EEM spectra of buffer solution containing oxygen NBs before and after US was applied; (E and F) EEM spectra of buffer solution containing oxygen NBs with 2 days storage before and after the application of US. The values represent the fluorescent intensities at 515 nm with excitation at 490 nm. (G) Error bars show the standard errors of 8 parallel samples. DO concentrations of oxygen NBs water and the control water were above 41.17 and 40.03 mg/L, respectively. APF was added after the US was applied. APF concentration was 1 μM).

DOI: 10.1021/acssuschemeng.5b01368
ACS Sustainable Chem. Eng. 2016, 4, 1347−1353

moderately high ROS level in the progenitor population sensitizes them to differentiation, and establishes a signaling role for ROS in the regulation of hematopoietic cell fate. In our research, the amount of ROS existed in the NB water was in the range of "oxidative window". Further investigation for ROS existence in the NB water can help us deeply understand the mechanism of NBs' physiological promotion effects.

Our results indicated that a small amount of ROS could be constantly detected in NB water with storage time. ROS have very short lifetimes, such as 1×10^{-9} s for ·OH,[37] and in the range from milliseconds to seconds at neutral pH values for $O_2^{\bullet-}$.[38] Thus, we concluded that ROS can be continuously produced in NB water. We also observed that both the DO concentration and the bubble number density of NB water decreases with storage time (Figure 2). These results indicate that NBs gradually disappear with storage. We hypothesize that the disappearance of NBs causes the constant production of ROS in water.

This hypothesis could be supported by the experimental results as following. As we know, the ultrasound could accelerate the aggregation process of the bubbles in an aqueous solution,[39] we tried to increase the disappearing number of NBs per unit time through the application of ultrasonic wave. First of all, we made it sure that the ultrasonic wave used in this study could only decrease but not increase the amount of NBs in water. We applied the ultrasonic wave to ultrapure water for 60 s and no bubbles could be detected through the nanoparticle tracking analysis method. For NB water, after the ultrasonic wave was applied for 60 s, the bubble number density significantly decreased (Figure S5). As can be seen in Figure 6, after the ultrasonic wave was applied to oxygen NBs water for 60 s, the fluorescence intensities of the NB solutions increased by 400, compared to those without ultrasonic wave pretreatment. The ultrasonic wave pretreatment did not affect the fluorescence intensity of control water. The above results showed that ROS was produced during NBs' disappearing process.

We also found that after ultrasonic wave application, the state of fast speed disappearance of NBs can last for a while. Having taken out the samples from the ultrasonic device, we waited for 30 min and then added APF in the samples. And the fluorescent increase of NB solution was about 100 (Figure S6). From Figure 6, after 2 days storage time, the statistical differences between the fluorescence intensities of oxygen NB water and the control water decreased from 40 to approximately 20. We applied the ultrasonic wave to the buffer containing oxygen NBs after 2 days storage time. The fluorescence intensities of the NB solutions increased by approximately 90, which is only one-fifth of the value we obtained just after generation of the oxygen NBs (Figure 6). From our experiments, we can conclude that the amount of ROS in NB water has positive correlation with the number of NBs and the decreasing speed of NBs number.

In recent years, many researchers have confirmed NBs' existence in solution on the basis of the results of their experiments, such as degassing,[40] relaxation time measurements,[1,29] transmission electron microscope observation,[41] measurement by dynamic light scattering method,[42] etc. Apart from the explanation of physiological promotion effect of NBs on seed germination, our results could also be used to prove the existence of NBs in the water. As disappearance of NBs is correlated to the free radical generation, the fluorescent intensity measurement can be a new method for the detection of existence of NBs in the water.

The production of ROS by NBs is a continual process. The stimulation on living organisms by NBs would last for a very long time, as is preferable for the metabolism of living organisms. Additionally, the number of NBs can be controlled to meet our needs through the operation of NB generator. When large amount of ROS are needed, different kinds of NBs like air NBs and oxygen NBs can also be used. Finally, the applications of NBs should not be limited to germination promotion. Because of their ability to produce ROS, it is anticipated that the prospects of NBs will be immense; however, much progress is still required. It is proposed that our study will act as a basis not only for applying NB technology to many areas of science and technology but also to developing new technology.

■ ASSOCIATED CONTENT

Supporting Information

The Supporting Information is available free of charge on the ACS Publications website at DOI: 10.1021/acssuschemeng.5b01368.

Schematic diagram for the measurement of superoxide radical in seeds, fluorescence responses of APF to gas mixture NB water, average relative absorbance values of endogenous ROS generation in barley seeds, distribution of endogenous ROS generation in barley seeds after 37 h of submerging time, effect of ultrasonic wave on the total bubble number concentration in gas mixture NB water, and effect of ultrasonic wave on the fluorescent intensities of the buffer containing oxygen NBs (PDF).

■ AUTHOR INFORMATION

Corresponding Authors

*Seiichi Oshita, E-mail: aoshita@mail.ecc.u-tokyo.ac.jp.

*Shu Liu. E-mail: liushu0313055@gmail.com. Tel.: 03-5841-5362. Fax: 03-5841-8174.

Notes

The authors declare no competing financial interest.

■ ACKNOWLEDGMENTS

A part of this research has been financially supported by Challenging Exploratory Research (25660202); Grant in Aid for Scientific Research (2402408) by JSPS; Council for Science, Technology and Innovation (CSTI); cross-ministerial Strategic Innovation Promotion Program (SIP); "Technologies for creating next-generation agriculture, forestry and fisheries" (funding agency: Bio-oriented Technology Research Advancement Institution, NARO), Japan; and Mayekawa Houonkai Foundation in 2013.

■ REFERENCES

(1) Ushikubo, F. Y.; Furukawa, T.; Nakagawa, R.; Enari, M.; Makino, Y.; Kawagoe, Y.; Shiina, T.; Oshita, S. Evidence of the existence and the stability of nano-bubbles in water. *Colloids Surf., A* **2010**, *361*, 31−37.

(2) Tsuge, H. *Micro- and Nanobubbles*; CMC: Tokyo, 2007; Chapter 2, pp 15−30 (In Japanese).

(3) Takahashi, M.; Kawamura, T.; Yamamoto, Y.; Ohnari, H.; Himuro, S.; Shakutsui, H. Effect of shrinking micro-bubble on gas hydrate formation. *J. Phys. Chem. B* **2003**, *107*, 2171−2173.

(4) Serizawa, A.; Inui, T.; Yahiro, T.; Kawara, Z. Laminarization of micro-bubble containing milky bubbly flow in a pipe. *3rd European-*

DOI: 10.1021/acssuschemeng.5b01368
ACS Sustainable Chem. Eng. 2016, 4, 1347−1353

Japanese Two-Phase Flow Group Meeting, Certosa di Pontignano, September 21−27, 2003.
(5) Chu, L. B.; Xing, X. H.; Yu, A. F.; Sun, X. L.; Jurcik, B. Enhanced treatment of practical textile wastewater by microbubble ozonation. *Process Saf. Environ. Prot.* **2008**, *86*, 389−393.
(6) Park, J.; Kurata, K. Application of microbubbles to hydroponics solution promotes lettuce growth. *Hortic. Technol.* **2009**, *19*, 212−215.
(7) Ebina, K.; Shi, K.; Hirao, M.; Hashimoto, J.; Kawato, Y.; Kaneshito, S. Oxygen and air nanobubble water solution promote the growth of plants, fishes, and mice. *PLoS One* **2013**, *8*, 1−7.
(8) Ago, K.; Nagasawa, K.; Takita, J.; Itano, R.; Morii, N.; Matsuda, K.; Takahashi, K. Development of an aerbic cultivation system by using a microbubble aeration technology. *J. Chem. Eng. Jpn.* **2005**, *38*, 757−762.
(9) Ohnari, H. Fisheries experiments of cultivated shells using micro-bubbles techniques, *J. Heat Transfer Soc. Jpn.* **2001**, *40*, 2−7 (In Japanese).
(10) Ohnari, H. Nakayama, T.; Nakata, A. Yamamoto, T. Generating mechanism of microbubble and its physiological characteristics, *Visualization Society of Japan*, **2003**, *23*, 105−106 (in Japanese), DOI: 10.3154/jvs.23.Supplement2_105.
(11) Ikeura, H.; Kobayashi, F.; Tamaki, M. Removal of residual pesticide, fenitrothion, in vegetables by using ozone microbubbles generated by different methods. *J. Food Eng.* **2011**, *103*, 345−349.
(12) Ikeura, H.; Kobayashi, F.; Tamaki, M. Removal of residual pesticides in vegetables using ozone microbubbles. *J. Hazard. Mater.* **2011**, *186*, 956−959.
(13) Inatsu, Y.; Kitagawa, T.; Nakamurai, N.; Kawasaki, S.; Nei, D.; Latiful Bari, Md.; Kawamoto, S. Effectiveness of stable ozone microbubble water on reducing bacteria on the surface of selected leafy vegetables. *Food Sci. Technol. Res.* **2011**, *17*, 479−485.
(14) Chu, L. B.; Xing, X. H.; Yu, A. F.; Zhou, Y. N.; Sun, X. L.; Jurcik, B. Enhanced ozonation of simulated dyestuff waste-water by microbubbles. *Chemosphere* **2007**, *68*, 1854−1860.
(15) Chu, L. B.; Yan, S. T.; Xing, X. H.; Yu, A. F.; Sun, X. L.; Jurcik, B. Enhanced sludge solubilization by microbubble ozonation. *Chemosphere* **2008**, *72*, 205−212.
(16) Liu, S.; Wang, Q. H.; Ma, H. Z.; Huang, P. K.; Li, J.; Kikuchi, T. Effect of micro-bubbles on coagulation flotation process of dyeing wastewater. *Sep. Purif. Technol.* **2010**, *71*, 337−346.
(17) Takahashi, M.; Ishikawa, H.; Asano, T.; Horibe, H. Effect of microbubbles on ozonized water for photoresist removal. *J. Phys. Chem. C* **2012**, *116*, 12578−12583.
(18) Takahashi, M.; Chiba, K.; Li, P. Formation of hydroxyl radicals by collapsing ozone microbubbles under strongly acidic conditions. *J. Phys. Chem. B* **2007**, *111*, 11443−11446.
(19) Li, P.; Takahashi, M.; Chiba, K. Enhanced free-radical generation by shrinking microbubbles using a copper catalyst. *Chemosphere* **2009**, *77*, 1157−1160.
(20) Tasaki, T.; Wada, T.; Fujimoto, K.; Kai, S.; Ohe, K. Degradation of methyl orange using short-wavelength UV irradiation with oxygen microbubbles. *J. Hazard. Mater.* **2009**, *162*, 1103−1110.
(21) Bailly, C.; El-Maarouf-Bouteau, H.; Corbineau, F. From intracellular signaling networks to cell death: the dual role of reactive oxygen species in seed physiology. *C. R. Biol.* **2008**, *331*, 806−814.
(22) Tomizama, S.; Imai, H.; Tsukada, S.; Simizu, T. The detection and quantification of highly reactive oxygen species using the novel HPF fluorescence probe in a rat model of focal cerebral ischemia. *Neuosci. Res.* **2005**, *52*, 304−313.
(23) Moritz, M.; Geszke-Moritz, M. The newest achievements in synthesis, immobilization and practical applications of antibacterial nanoparticles. *Chem. Eng. J.* **2013**, *228*, 596−613.
(24) Ishibashi, Y.; Tawaratsumida, T.; Zheng, S. H.; Yuasa, T.; Iwaya-Inoue, M. NADPH Oxidases act as key enzyme on germination and seeding growth in barley (Hordeum vulgare L.). *Plant Prod. Sci.* **2010**, *13*, 45−52.
(25) Muller, K.; Linkies, A.; Vreeburg, R. A. M.; Fry, S. C.; Krieger-Liszkay, A.; Leubner-Metzger, G. In vivo cell wall loosening by hydroxyl radicals during cress seed germination and elongation growth. *Plant Physiol.* **2009**, *150*, 1855−1865.
(26) Naredo, M. E. B.; Juliano, A. B.; Lu, B. R.; de Guzman, F.; Jackson, M. T. Responses to seed dormancy-breaking treatments in rice species (Oryza L.). *Seed Sci. Technol.* **1998**, *26*, 675−689.
(27) Ogawa, K.; Iwabuchi, M. A mechanism for promoting the germina- tion of Zinnia elegans seeds by hydrogen peroxide. *Plant Cell Physiol.* **2001**, *42*, 286−291.
(28) Ishibashi, Y.; Tawaratsumida, T.; Kondo, K.; Kasa, S.; Sakamoto, M.; Aoki, N.; Zheng, S. H.; Yuasa, T.; Iwaya-Inoue, M. Reactive oxygen species are involved in gibberellin/Abscisic Acid signaling in barley aleurone cells. *Plant Physiol.* **2012**, *158*, 1705−1714.
(29) Liu, S.; Kawagoe, Y.; Makino, Y.; Oshita, S. Effects of nanobubbles on the physicochemical properties of water: the basis for peculiar properties of water containing nanobubbles. *Chem. Eng. Sci.* **2013**, *93*, 250−256.
(30) Zimmerman, W. B.; Tesař, V.; Bandulasena, H. C. H. Towards energy efficient nanobubble generation with fluidic oscillation. *Curr. Opin. Colloid Interface Sci.* **2011**, *16* (4), 350−356.
(31) Bunkin, N. F.; Shkirin, A. V.; Ignatiev, P. S.; Chaikov, L. L.; Burkhanov, I. S. Nanobubble clusters of dissolved gas in aqueous solutions of electrolyte. I. Experimental proof. *J. Chem. Phys.* **2012**, *137*, 054706.
(32) Setsukinai, K.-i.; Urano, Y.; Kakinuma, K.; Majima, H. J.; Nagano, T. Development of novel fluorescence probes that can reliably detect reactive oxygen species and distinguish specific species. *J. Biol. Chem.* **2003**, *278*, 3170−3175.
(33) Chapple, I. L. C.; Matthews, J. B. The role of reactive oxygen and antioxidant species in periodontal tissue destruction. *Periodontology* **2007**, *43*, 160−232.
(34) Kranner, I.; Roach, T.; Beckett, R. P.; Whitaker, C.; Minibayeva, F. V. Extracellular production of reactive oxygen species during seed germination and early seedling growth in Pisumsativum. *J. Plant Physiol.* **2010**, *167*, 805−811.
(35) Owusu-Ansah, E.; Banerjee, U. Reactive oxygen species prime Drosophila haematopoietic progenitors for differentiation. *Nature* **2009**, *461*, 537−541.
(36) Owusu-Ansah, E.; Yavari, A.; Mandal, S.; Banerjee, U. Distinct mitochondrial retrograde signals control the G1-S cell cycle checkpoint. *Nat. Genet.* **2008**, *40*, 356−361.
(37) Donoghue, M. A.; Xu, X.; Bernlohr, D. A.; Arriaga, E. A. Capillary electrophoretic analysis of hydroxyl radicals produced by respiring mitochondria. *Anal. Bioanal. Chem.* **2013**, *405*, 6053−6060.
(38) Chen, X. J.; West, A. C.; Cropek, D. M.; Banta, S. Detection of the Superoxide Radical Anion Using Various Alkanethiol Monolayers and Immobilized Cytochrome c. *Anal. Chem.* **2008**, *80*, 9622−9629.
(39) Masuda, N.; Maruyama, A.; Eguchi, T.; Hirakawa, T.; Murakami, Y. Influence of Microbubbles on Free Radical Generation by Ultrasound in Aqueous Solution: Dependence of Ultrasound Frequency. *J. Phys. Chem. B* **2015**, *119*, 12887−12893.
(40) Häbich, A.; Ducker, W.; Dunstan, D. E.; Zhang, X. H. Do Stable Nanobubbles Exist in Mixtures of Organic Solvents and Water ? *J. Phys. Chem. B* **2010**, *114*, 6962−6967.
(41) Uchida, T.; Oshita, S.; Ohmori, M.; Tsuno, T.; Soejima, K.; Shinozaki, S.; Take, Y.; Mitsuda, K. Transmission electron microscope observations of nanobubbles and their capture of impurities in wastewater. *Nanoscale Res. Lett.* **2011**, *6*, 295.
(42) Najafi, A. S.; Drelich, J.; Yeung, A.; Xu, Z. H.; Masliyah, J. A novel method of measuring electrophoretic mobility of gas bubbles. *J. Colloid Interface Sci.* **2007**, *308*, 344−350.

DOI: 10.1021/acssuschemeng.5b01368
ACS Sustainable Chem. Eng. 2016, 4, 1347−1353